FIRST-PRINCIPLES CALCULATIONS OF C_2H_4 GAS ADSORPTION IN TRANSFORMER OIL BY PD-DOPED GRAPHDIYNE

Haidan LIN[1], Zilong ZHANG[2], Daiyong YANG[3], Shouxue LI[4], Haifeng ZHANG[5,*]

Based on the first-principles density-functional theory (DFT), the electronic structure evolution of Pd clusters doped with different numbers of Pd atoms on the surface of palladium-doped graphene-like carbon (GDY) and its effect on the adsorption behaviour of ethylene (C_2H_4) molecules were investigated. The results show that GDY, as a two-dimensional carbon substrate, has good stability to Pd single atoms and cluster active sites, and the Pd_4/GDY configuration containing four Pd atoms has the strongest adsorption capacity for C_2H_4. This study lays an insistent foundation for the online monitoring of C_2H_4 and other dissolved gases in transformer oil.

Keywords: graphitic; acetylene; DFT; doped; dissolved gas; C_2H_4

1. Introduction

With the increasing demand for electrical power consumption in society, the stability of power systems has become an indispensable and crucial component of social development [1]. Power transformers hold a pivotal role as indispensable components in power systems, serving the critical purpose of facilitating voltage conversion in electrical transmission lines. The operational condition of power transformers holds paramount significance in ensuring the secure and stable functioning of the entire power grid infrastructure. From a chemical structure perspective, transformer oil, which is used in power transformers, is mainly composed of hydrocarbon compounds. However, with prolonged operation of transformers, partial discharge phenomena are unavoidable [2]. The breakage of C-C and C-H bonds can be caused because of these discharges cases in the transformer

[1] PhD, Electric Power Research Institute, State Grid Jilin Electric Power Co., Ltd., Changchun, 130012, China, a125790709@163.com
[2] Mr., School of Chemistry Engineering, Northeast Electric Power University, Jilin 132012, China, zilongzhang_neepu@163.com
[3] Eng., Jilin Electric Power Research Institute Co., Ltd., Changchun, 130012, China; sr17662744213@163.com
[4] Eng., Electric Power Research Institute, State Grid Jilin Electric Power Co., Ltd., Changchun, 130012, China, x13629890704@163.com
[5] Prof., School of Chemistry Engineering, Northeast Electric Power University, Jilin 132012, China, zhfeepu@163.com

oil, and the small amounts of reactive hydrogen atoms and unstable hydrocarbon radicals were generated, thereby producing characteristic gases such as hydrogen (H_2), ethylene (C_2H_4), methane (CH_4), and others. Empirical investigations have demonstrated a strong correlation between the presence of dissolved gases in transformer oil and the occurrence of transformer faults [3]. Given the correlation between characteristic gases and discharge faults, the type and severity of discharge faults can be diagnosed effectively by utilizing the analysis of dissolved gases (DGA) [4,5]. Among them, ethylene (C_2H_4) holds significant importance as a typical decomposition product for assessing faults in oil-immersed transformers [6].

Gas sensors, as an important method for gas detection [7,8], have gained wide attention in the power system because of its high sensitivity, small size, and low cost [9]. In recent times, there has been a remarkable surge in the fascination among researchers regarding two-dimensional (2D) materials. This heightened interest can be attributed to their exceptional qualities, such as high carrier mobility, outstanding thermal and electrical conductivity, customizable bandgap, and distinctive optical characteristics [10]. The chemical arrangement of graphdiyne (GDY), a newly discovered two-dimensional planar carbon material, depends on the bonding between its sp and sp^2 hybridization states. A large number of carbon-based bonds, a high level of porosity, an evenly scattered pore configuration, and a customizable electronic structure are characteristics of GDY. It also possesses great qualities including a large specific surface area, thermal stability, eco-friendliness, photothermal effect, photoluminescence, etc. [11,12], according to research. The distinct alkyne bonding structure of graphene, especially when compared to other carbon materials, interacts strongly with metal ions, opening up a wide range of potential applications in the field of transformer oil. However, as a typical 2D material, graphdiyne is still in the computational and simulation stage regarding gas molecule detection, and related research is relatively limited. Nevertheless, some studies have shown promising response characteristics of graphdiyne towards formaldehyde. The strong interaction between graphdiyne and the highly electronegative formaldehyde leads to electron cloud shifting within the graphdiyne carbon framework, resulting in an increase in electron cloud density and a decrease in resistance [13], leading to a reduction in the measured current value. Additionally, theoretical research indicates that graphdiyne exhibits strong binding energy with gas molecules such as trimethylamine and dimethylamine [14]. The bandgap structure of graphene can be altered by gas adsorption, which can serve as an indicator for gas detection [15]. Furthermore, doping cardopedbon materials with noble metals (such as Au, Ag, Pd, and Pt [16]) the adsorption and sensing performance of the adsorption system can be effectively enhanced towards gas molecules, and the detection sensitivity of sensors were significantly improved. Noble metals are considered excellent super-dopants for enhancing gas adsorption and sensing performance due to their outstanding catalytic properties and chemical

reactivity in gas interactions [17-19]. However, to the best of our knowledge, research on noble metal-doped graphene concerning the adsorption or sensing behavior towards typical characteristic gases in transformer oil is relatively limited. Therefore, it is of great significance to study the electronic performance of noble metal-doped graphene and its gas sensing characteristics towards characteristic gases in transformer oil [20-22].

The density functional theory (DFT) is used for the first-principles calculations that form the basis of this investigation. We investigated the ethylene (C_2H_4) adsorption behavior on Pd-doped graphdiyne (Pd_n/GDY, n = 1-6) systems with different numbers of Pd clusters. Ethylene is a distinctive gas that is frequently dissolved in transformer oil. Prior to and during the adsorption of Pd_n/GDY and C_2H_4, the structural alterations, adsorption energies, charge transfer, densities of states, differential charge densities, and molecular orbital development were examined. We clarified the interactions between the substrate and the adsorbed gas. A novel gas sensing material was provided for the detection of dissolved gases in transformer oil, which establishes a basis for evaluating the operational condition of power transformers. Through further advancements in this work, the underlying mechanisms were deeper understanded, the stable operation and fault diagnosis of power systems was supported valuably.

2. Computational details

In this paper, all computational analyses and calculations were conducted utilizing the Vienna Ab initio Simulation Package (VASP) within the context of the density functional theory (DFT) framework. In this study, the Perdew-Burke-Ernzerhof (PBE) exchange-correlation functional, which belongs to the generalized gradient approximation (GGA) family, was employed to evaluate the exchange-correlation energy. Dispersion contributions were introduced through the D3 approach. Furthermore, the treatment considered the influence of spin polarization during the computational procedures. The interaction between atomic cores and valence electrons were explored with projector-augmented wave (PAW) method of electronic pseudopotential calculations and the valence monoelectronic states expanded as plane waves with a cutoff kinetic energy of 450 eV. In order to enhance the accuracy of adsorption energy calculations, we implemented the DFT-D method proposed by Grimme. To prevent spurious interactions between adjacent cells, an intrinsic graphdiyne (GDY) structure with dimensions of 1.92 nm × 1.92 nm × 1.5 nm was constructed, interleaved by 15 Å of vacuum, imposing periodic boundary conditions. Throughout the calculations, symmetry considerations were applied, and the Brillouin zone integration was performed using the Gamma point sampling scheme with a k-point grid of 2×2×1. A dipole correction was employed along the z direction. Geometrical optimization was carried out until the forces on each atom

converged to within 0.01 eV $Å^{-1}$, and self-consistency was achieved with a convergence threshold of 10^{-7} eV, ensuring the precision of the obtained results.

The combined energy of Pd and GDY is calculated as:

$$E_b = E_{(Pd_n-GDY)} - E_{(GDY)} - n \times E_{(Pd-bulk)} \quad (1)$$

As defined in Equation 1， where E_b represents the binding energy, $E_{(Pd_n-GDY)}$ represents the overall energy of the configuration, $E_{(GDY)}$ represents the GDY substrate energy, and $E_{(Pd-bulk)}$ represents the energy of a single atom in the bulk phase Pd.

The adsorption energy of gas molecules is calculated as:

$$E_{ads} = E_{total} - E_{(Pd_n-GDY)} - E_{(C_2H_4)} \quad (2)$$

In the formula, E_{ads} signifies the adsorption energy of substrates adsorbed on the adsorption site (As defined in Equation 2), E_{total} represents the overall energy of the system subsequent to the adsorption of molecules, $E_{(Pd_n-GDY)}$ denotes the reference energy or baseline energy, and $E_{(C_2H_4)}$ designates the energy of C_2H_4 molecules.

3. Results and discussion

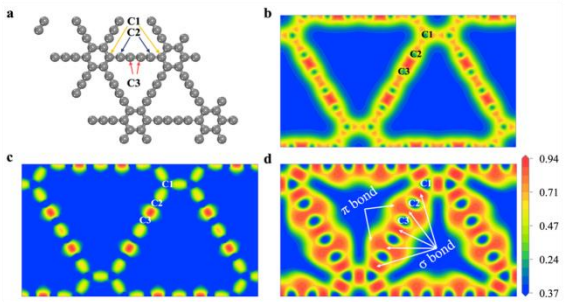

Fig. 1. (a) Graphdiyne model (b-d) Electronic state distribution

Firstly, the graphdiyne (GDY) substrate was constructed, and the stable model was obtained by utilizing in this study and performing structural optimization based on the aforementioned computational parameters as depicted in Fig. 1. In this model, the lattice constant of the unit cell was verified to be 19.2 Å, consistent with previously reported results in the literature [23]. Within the graphdiyne structure, three types of carbon atoms denoted as C_1, C_2, and C_3, were identified. We conducted calculations and obtained the bond lengths of C_{sp2}-C_{sp2}, C_{sp2}-C_{sp}, and C_{sp}-C_{sp} bonds, which were found to be 1.456 Å, 1.422 Å, and 1.243/1.361 Å [24], respectively, in good agreement with literature reports [25]. Due to the unique electronic properties of graphdiyne, the presence of sp-hybridized carbon atoms allows for free rotation of the P_x-P_y π/π* orbitals within the plane, perpendicular to the direction of the C≡C bond. As a result, the π/π* orbitals of the

C≡C bond can consistently orient toward the anchored metal monomers, offering the potential for anchoring metal monomers on the graphdiyne surface.

Fig. 2 presents the optimized structures of Pd (Pd_n/GDY, n = 1-6) atoms adsorbed on graphdiyne was exhibited, showcasing the changes in the two-dimensional planar structure of the graphdiyne system upon the introduction of varying numbers of Pd atoms. From the figure, it can be observed that the addition of different quantities of Pd atoms induces significant modifications in the two-dimensional structure of the graphdiyne system. Particularly, when the number of Pd atoms is n = 4-6, a noticeable upward protrusion of neighboring carbon atoms in the carbon substrate can be observed, indicating a significant interaction between Pd and graphdiyne. This raised interface structure implies that the porous structure of graphdiyne can effectively anchor Pd atoms, their stability were enhanced on the graphdiyne substrate. Analyzing the Pd_n/GDY systems with different numbers of Pd atoms, it is found that in the Pd_1/GDY structure, when a single Pd atom is introduced into the graphdiyne system, it forms four Pd-C bonds with neighboring sp carbon atoms. The bond lengths of the Pd-C bonds range from 2.05 to 2.15 Å, indicating the covalent nature of the Pd-C bonds, consistent with reported results in the literature [26]. Additionally, the introduction of Pd atoms also leads to a significant variation in the lengths of certain C-C bonds within the graphdiyne system, shifting from approximately 1.24 Å before Pd adsorption to around 1.30 Å after adsorption, signifying a rearrangement of the electronic structure, particularly in the vicinity of the Pd atoms in the entire graphdiyne system.

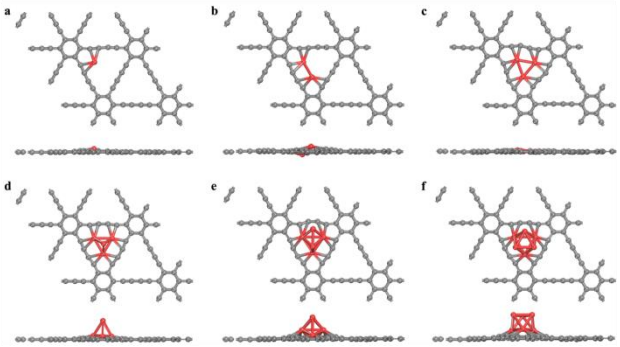

Fig. 2. Effect of GDY on the adsorption configuration (Pd_n/GDY, n = 1-6) of Pd_1-Pd_6

In the figures 2b-f, the structural models of graphdiyne systems with 2-6 Pd atoms were depicted. When two Pd atoms form a cluster, a different Pd coordination state emerges compared to the Pd_1/GDY system with a single Pd atom. One Pd atom forms three Pd-C bonds with the surrounding Pd atoms, while the other Pd atom forms four Pd-C bonds, and the two Pd atoms are connected by a Pd-Pd bond. Computed results indicate a bond length of approximately 2.76 Å between the two Pd atoms, displaying typical characteristics of a metal bond. With an increasing number of atoms in the Pd cluster, a more complex coordination environment is

observed. The maximum bond length of the Pd-Pd bond decreases from approximately 2.76 Å in Pd_2/GDY to around 2.55 Å in Pd_6/GDY, and the deformation of graphdiyne becomes more pronounced, deviating from the planar structure. According to relevant studies [27], the adsorption of metal atoms on the graphdiyne surface leads to hybridization of the valence electrons of these metal atoms. This hybridization occurs not only with the P_z orbitals of the carbon atoms in graphdiyne but also extends to the P_x and P_y orbitals. This synergistic effect strengthens the bonding between the metal atoms and graphdiyne, thereby inducing the deformation of graphdiyne.

Fig. 3, plotted based on the calculated results, the adsorption energies of the six Pd_n/GDY systems were displayed. From the figure, it can be observed that all six adsorption structures exhibit relatively high adsorption energies at the large angular sites of the graphdiyne structure. As the number of Pd atoms increases from 1 to 6, the adsorption energies evolve as follows: -2.82, -2.76, -3.02, -2.76, -2.76, -2.75 eV, forming an inverted volcano-shaped curve. Among them, the Pd_3/GDY system exhibits the lowest adsorption energy, indicating that among all the adsorption structures, the Pd_3 adsorption structure is thermodynamically the most stable. Relevant literature suggests that among numerous possible adsorption sites [28], the adsorption energy is strongest for monatomic noble metal adsorption at the center of the triangular large pore in graphdiyne. This is because the noble metal atom forms strong covalent bonds with the C≡C bonds surrounding the large pore upon adsorption, making it difficult for the metal atom to migrate, thus favoring the stable presence of the metal atom.This viewpoint was further verified about the covalent nature of the Pd-C bonds in this study.

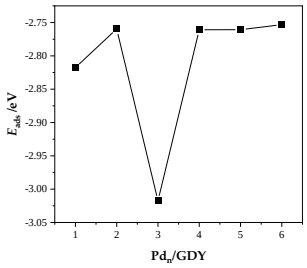

Fig. 3. Effect of GDY on adsorption energy of Pd_1-Pd_6

According to the results presented in Fig. 4, we can observe significant charge transfer between the Pd atoms and GDY in the Pd_n/GDY systems, leading to the formation of strong covalent bonds and high oxidation states for some Pd atoms. Structural stability was maintained by this charge transfer mechanism, while electron-rich ethyne/ethylene molecules were adsorbed by Pd atoms efficiently.

Specifically, we conducted a quantitative analysis of the electronic transfer between Pd and GDY in several structures. When a single Pd atom is doped into the graphdiyne, the charge mainly accumulates at the central position of the Pd-C

bonds. At this point, the outer d-orbital electrons of the Pd atom exhibit a significant outflow trend. As the number of Pd atoms in the cluster increases, this trend weakens relatively. For example, when the number of atoms in the Pd cluster is 3, the amount of electron outflow from the Pd atom at site 1 decreases from the previous -0.2685 e to -0.1999 e, indicating that 0.0686 electrons remain untransferred. The electron loss during the process of increasing the number of Pd atoms in the cluster from 1 to 3 does not show a clear linear relationship with the adsorption energy. In the adsorption configurations with a larger number of Pd atoms, even electron inflow can be observed for Pd atoms at sites 4, 5, and 6. This suggests that as the coordination environment around the Pd atoms becomes more complex, the arrangement of outer-shell electrons of the Pd atoms is subject to more restrictions, resulting in multipolar electron flow characteristics. Eventually, these Pd atoms form larger Pd nanoclusters, shielding the interaction with GDY.

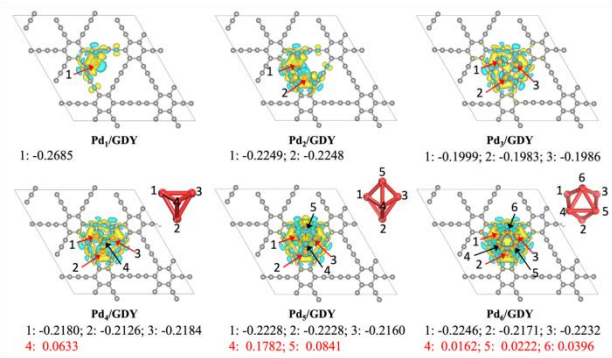

Fig. 4. Pd_n-GDY system differential density charge and electron transfer

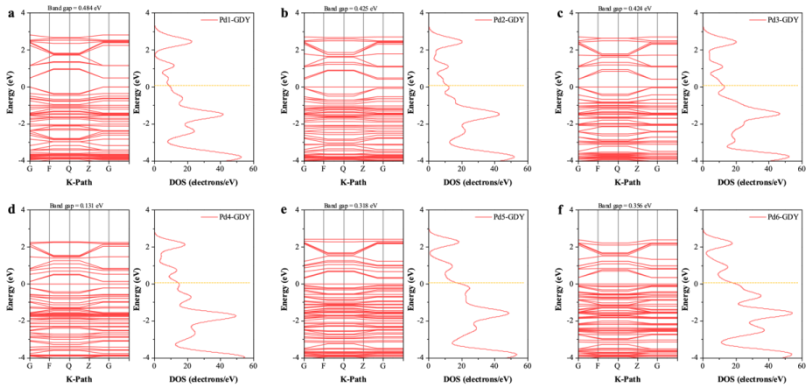

Fig. 5. Pd_n/GDY systems can have structure and state density

Based on the band structure and density of states (DOS) results shown in Fig. 5, the distribution of orbital contributions from Pd atoms can further be confirmed in different systems. Figure 5a on the left displays the atomic orbital contribution distribution of Pd atoms in the Pd_1/GDY system, while the right side

shows the visualized band structure of the system. From Figure 5a, it is evident that the band structure of the Pd_1/GDY system exhibits two non-intersecting curves near the Fermi level (represented by a dashed line), with a bandwidth of 0.484 eV. Figure 5b presents the DOS plot for Pd_2/GDY, which shows a reduced bandwidth of 0.425 eV compared to Pd_1/GDY. Similarly, Pd_3/GDY exhibits a bandwidth of 0.424 eV. However, as the number of Pd atoms increases to 4, 5, and 6, the bandwidth significantly decreases to 0.131, 0.318, and 0.356 eV, respectively. This observation suggests a decrease in the energy barrier for electron transfer from the valence band to the conduction band, making the transfer easier and increasing the conductivity of the system.

By comparing the changes in conductivity among the Pd_{1-6}/GDY systems, it can be inferred that Pd clusters with an atomic number ranging from 4 to 6 may exhibit better performance. Moreover, a comprehensive examination was conducted concerning the superposition of the highest occupied state and the lowest unoccupied state at the K-point position within the Pd_{1-6}/GDY systems. The findings unveiled that the K-point values corresponding to the minimum of the conduction band and the maximum of the valence band are degenerate, signifying the presence of a degenerate band structure at the K-point. This direct bandgap characteristic suggests that the Pd_4/GDY substrate may possess superior substrate molecule adsorption capabilities. In this case, the binding of Pd atoms to the outer-shell electrons is reduced, potentially resulting in more active adsorption and gas sensitivity performance.

In conclusion, through the analysis of band structures and density of states, the information about the orbital contribution distribution of Pd atoms in different systems can be obtained, and the Pd_4/GDY substrate can be speculated about the possess better adsorption performance and gas sensitivity. These findings provide important clues for further understanding the electronic properties and adsorption behavior of the Pd_n/GDY system.

Based on the adsorption structure shown in Fig. 6, it can be observed that the optimized ethylene (C_2H_4) molecule is adsorbed parallel to the Pd_n/GDY surface, aligned with the top of the Pd atoms. The measured results indicate that the adsorption distances of the optimized C_2H_4 molecule on the Pd_n/GDY surface are 2.20, 2.15, 2.18, 2.14, 2.18, and 2.13 Å for different Pd clusters. The Pd_n/GDY substrate undergoes slight deformation, suggesting that chemical adsorption is the predominant interaction between C_2H_4 and Pd_n/GDY. To substantiate this conclusion, we performed an examination employing molecular orbital theory, focusing on the highest occupied molecular orbital (HOMO) and lowest unoccupied molecular orbital (LUMO). Figure 7 displays the HOMO and LUMO distributions of the Pd_n/GDY material before and after C_2H_4 adsorption, with the energy gap widths indicated.

Drawing upon the outcomes depicted in Fig. 7, it can be observed that there is almost no change in the energy gap before and after C_2H_4 adsorption on Pd_1/GDY and Pd_2/GDY materials. This implies that the extent of electronic transfer for C_2H_4 is relatively low on these two substrates, making the adsorption relatively challenging. However, as the number of Pd atoms increases, the adsorption behavior undergoes a significant change. In the Pd_3-GDY to Pd_6-GDY systems, the energy gap after C_2H_4 adsorption noticeably decreases, indicating enhanced adsorption of C_2H_4. It is noteworthy that when the number of Pd atoms in the cluster is 4, the energy gap after C_2H_4 adsorption on Pd_4/GDY substrate is only 0.0003 eV, which is 20 times smaller than the gap before adsorption. Clearly, at this point, the adsorption strength between the adsorbate and the substrate is the strongest, and electronic transfer becomes more pronounced.

In conclusion, based on the computational results, we can conclude that in the Pd_n/GDY systems, with an increasing number of Pd atoms, the adsorption of C_2H_4 molecules is facilitated, leading to a reduction in the energy gap and indicating more pronounced electronic transfer. Specifically, in the Pd_4/GDY system, the energy gap for C_2H_4 adsorption significantly decreases, suggesting the highest adsorption strength. This finding further supports the previous speculation that Pd_4/GDY substrate exhibits superior adsorption performance and gas-sensing capabilities.

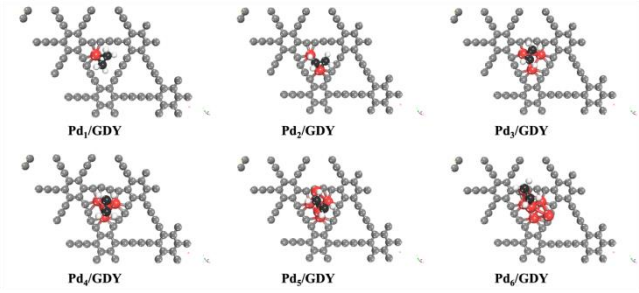

Fig. 6. Adsorption configuration of ethylene on Pd_n/GDY

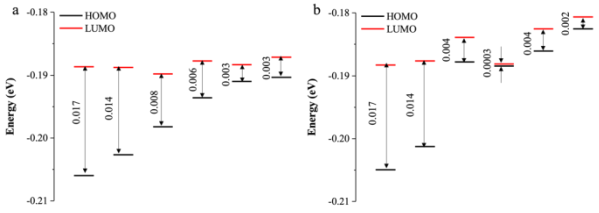

Fig. 7. HOMO and LUMO distribution before and after C_2H_4 adsorption (a) before adsorption, (b) post-adsorption.

Drawing upon the outcomes depicted in Fig. 8, we can further substantiate the previous conclusions. The adsorption energies of C_2H_4 vary as the number of

Pd clusters evolves from 1 to 6, with values of -0.48, -0.18, -0.28, -0.58, -1.50, and -1.38 eV, respectively. These results indicate that different energies are released during the adsorption process of C_2H_4, with the Pd_4/GDY system exhibiting the optimal performance. Specifically, the adsorption of C_2H_4 on the Pd_4/GDY substrate is thermodynamically the most stable.

Based on the analysis of C_2H_2 adsorption on the Pd_n/GDY system, the feasibility of using Pd_n/GDY-based gas sensors were initially confirmed for online monitoring of dissolved gases in transformer oil. The observation of a high adsorption capacity in the Pd_4/GDY substrate suggests its favorable suitability as an efficient adsorbent for dissolved gases in transformer oil. Consequently, this characteristic facilitates the effective utilization of gas sensors in online monitoring systems, enabling continuous and proficient detection of dissolved gases. By capitalizing on the adsorption capabilities of the Pd_4/GDY substrate, gas sensors can adeptly capture and analyze dissolved gases, providing valuable real-time data for the purpose of transformer condition monitoring.

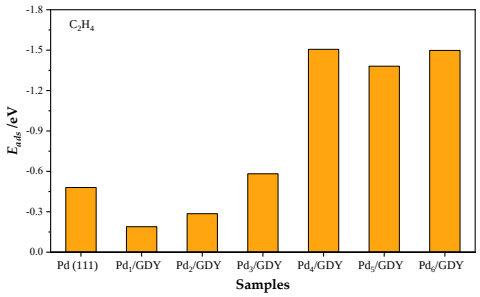

Fig. 8. Adsorption energy of ethylene on Pd_n/GDY system

According to the density of states (DOS) distribution plot of the C_2H_4 adsorption system shown in Fig. 9, the overall peak of the total DOS after C_2H_4 adsorption does not exhibit significant changes but rather shows a slight leftward shift. However, the peak at the Fermi level shows a slight decrease. This is consistent with the trend of band lowering observed after adsorption.

The orbital overlap between the Pd atoms on the GDY surface and the atomic orbitals of the C_2H_4 molecule following C_2H_4 adsorption is shown as a density of states (DOS) distribution in Fig. 10. The graphic makes it clear that on $Pd_{4\text{-}6}$/GDY, the 4d orbitals of Pd atoms, the 2p orbitals of C atoms, as well as the 1s orbitals of H atoms in the C_2H_4 molecule, significantly overlap. In the Pd_4/GDY system, the overlap between C and Pd is particularly strong. This further supports the prior findings on the charge transfer and bandgap changes during C_2H_4 adsorption on Pd_4/GDY and points to a significant interaction between the Pd atoms in the Pd_4/GDY system and the C_2H_4 molecule.

Detailed information was provided about these findings of the electronic density distribution and the interaction between atomic orbitals in the Pd_4/GDY

system upon C_2H_4 adsorption. This further supports the feasibility of utilizing Pd_4/GDY as a gas sensing material for online monitoring of dissolved gases in transformer oil. Moreover, these results offer valuable insights for the optimization of sensor performance in this application.

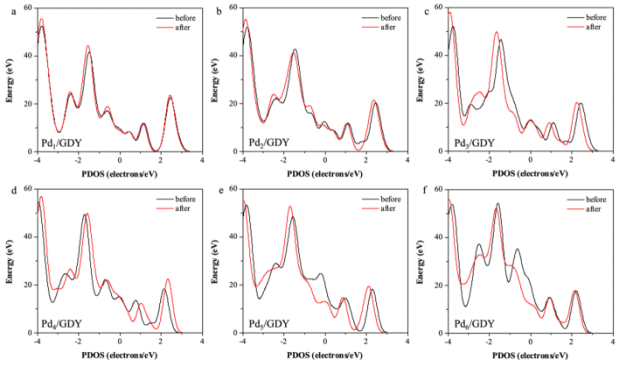

Fig. 9. Ethylene adsorbs DOS before and after on the Pd_n/GDY system

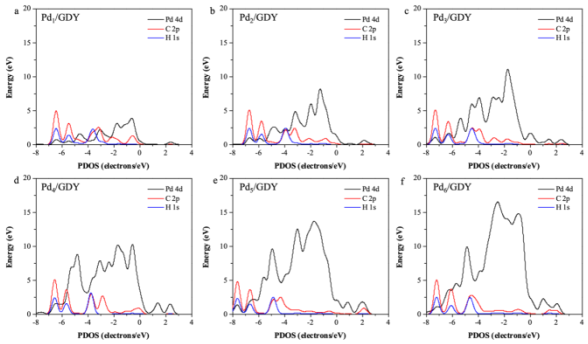

Fig. 10. Ethylene adsorbs PDOS before and after Pd_n/GDY system

The pattern of electron transfer between the substrate and the adsorbed molecule is shown by the electron difference density map in Figure 11, where red areas denote electron depletion and blue areas electron buildup. Elevated electron density may be seen in the bonding areas of ethylene (C_2H_4). It is possible to quantify the amount of electrons transferred from C_2H_4 to Pd by doing a Bader charge analysis and counting the total number of electrons lost by the complete C_2H_4 molecule. 0.050, 0.031, 0.033, 0.066, 0.046, and 0.042 eV, respectively, are the predicted electron transfer values for C_2H_4 in each system.

Changes in conductivity have an essential theoretical basis in electron transport. If the findings from Fig. 11 are combined, it is possible to deduce that, with the exception of the $Pd_{1\text{-}2}$/GDY systems, the degree of conductivity change upon adsorption rises in proportion to the rate of electron transfer for the other systems. For these four systems, the order of conductivity change is as follows, from highest to lowest: C_2H_4-Pd_4/GDY > C_2H_4-Pd_3/GDY > C_2H_4-$Pd_{5\text{-}6}$/GDY. Fig.

7 shows that, compared to the Pd_4/GDY system, the region capable of receiving charge in the lowest unoccupied molecular orbital (LUMO) is noticeably smaller, resulting in less pronounced changes in conductivity, even though the Pd_3/GDY and $Pd_{5\text{-}6}$/GDY systems exhibit significant changes in conductivity during the adsorption process.

In conclusion, using estimates of the electron difference density, a qualitative investigation of electron transfer in the adsorption systems was further carried out. The findings show that the extent of electron transfer is connected with the degree of conductivity change, and that the band structure and the quantity of charge transfer have an impact on the magnitude of conductivity change in various systems. These results offer crucial hints for a deeper comprehension of the conductivity performance and adsorption behavior of the Pd_n/GDY systems.

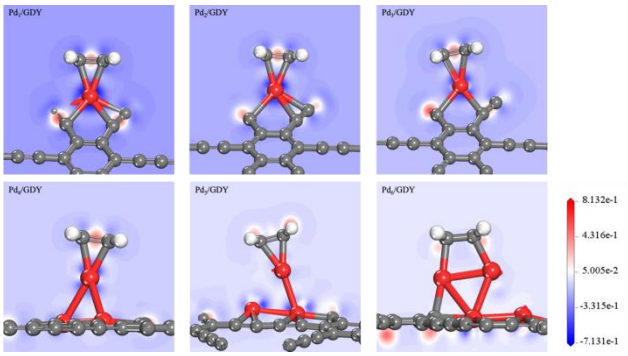

Fig. 11. The differential charge density of ethylene adsorbed on Pd_n/GDY systems

4. Conclusions

In this paper, the adsorption behavior of characteristic gas C_2H_4 in typical transformer oil was investigated by analyzing Pd clusters with different numbers of Pd atoms doped in graphdiyne (GDY) using first-principles theory. Several conclusions can be put forward: I). GDY, a new two-dimensional carbon-based substrate, demonstrates good stability toward Pd single atoms and clusters as active centers. It also has the capacity to modify the electronic structure of Pd active centers, including the band gap, energy level, and ethylene adsorption capabilities. II). Pd_1-P_6 clusters are stable when joined with GDY, and Pd_4-P_6/GDY exhibits lower band widths and HOMO-LUMO energy gaps, suggesting their potential as sensors. This was discovered by evaluating the doped substrate structures and binding energies. III). Pd cluster-doped graphene considerably affects C_2H_4 adsorption, particularly Pd_4/GDY, which has high C_2H_4 adsorption and electron-accepting properties. IV). Graphene that has been doped with Pd has good conductivity, especially Pd_4/GDY, which may take on more charge during the adsorption process.

In summary, this study highlights that Pd_n/GDY materials are promising candidates for adsorbing harmful gases generated during the decomposition of transformer oil. The findings hold significant implications for the application of gas sensors in power systems and provide valuable references for future researchers in this field.

Acknowledgement

This project is supported by funds from the Science and Technology Project of State Grid Jilin Province Electric Power Co., Ltd. (2022JBGS-01).

R E F E R E N C E S

[1] *Adebayo I, Sun Y.* New performance indices for voltage stability analysis in a power system. Energies, 2017, 10(12): 2042.

[2] *Callender G, Lewin P L.* Modeling partial discharge phenomena. IEEE Electrical Insulation Magazine, 2020, 36(2): 29-36.

[3] *Li J, Li G, Hai C, et al.* Transformer fault diagnosis based on multi-class AdaBoost algorithm. IEEE Access, 2021, 10: 1522-1532.

[4] *Ali M S, Omar A, Jaafar A S A, et al.* Conventional methods of dissolved gas analysis using oil-immersed power transformer for fault diagnosis: A review. Electric Power Systems Research, 2023, 216: 109064.

[5] *Kim Y, Kweon D, Park T, et al.* Classification of fault and failure types determined by dissolved gas analysis for transformers. Journal of Electrical Engineering & Technology, 2019, 14: 1665-1674.

[6] *Toldra-Reig F, Serra J M.* Potentiometric C_2H_4-Selective Detection on Solid-State Sensors Activated with Bifunctional Catalytic Nanoparticles. Chemosensors, 2021, 9(10): 274.

[7] *Zhang Q, Zhou Q, Lu Z, et al.* Recent advances of SnO_2-based sensors for detecting fault characteristic gases extracted from power transformer oil. Frontiers in chemistry, 2018, 6: 364.

[8] *Jiang T, Zhang W, Zhang T, et al.* Adsorption and gas-sensing performances of C_2H_2, C_2H_4, CO, H_2 in transformer oil on Pt-doped $MoTe_2$ monolayer: A DFT study. Physica E: Low-dimensional Systems and Nanostructures, 2023, 146: 115568.

[9] *Mahanta D K, Laskar S.* Investigation of transformer oil breakdown using optical fiber as sensor. IEEE Transactions on Dielectrics and Electrical Insulation, 2018, 25(1): 316-320.

[10] *Zhao Y, Chai L, Yan X, et al.* Characteristics, properties, synthesis and advanced applications of 2D graphdiyne versus graphene. Materials Chemistry Frontiers, 2022, 6(5): 528-552.

[11] *Li Y, Xu L, Liu H, et al.* Graphdiyne and graphyne: from theoretical predictions to practical construction. Chemical Society Reviews, 2014, 43(8): 2572-2586.

[12] *Zhao Y, Yang N, Yao H, et al.* Stereodefined codoping of sp-N and S atoms in few-layer graphdiyne for oxygen evolution reaction. Journal of the American Chemical Society, 2019, 141(18): 7240-7244.

[13] *Ivanovskii A L.* Graphynes and graphdyines. Progress in Solid State Chemistry, 2013, 41(1-2): 1-19.

[14] *Akbudak S, Ellialtıoğlu M R.* Effect of core electrons in defining the total energy, correlation energy, and binding energy of graphene, graphite, and diamond: a first-principles study. Journal of Superconductivity and Novel Magnetism, 2018, 31: 3097-3104.

[15] *Inoue S, Tomita Y, Kokabu T, et al.* Principles of detection mechanism for adsorbed gases using carbon nanotube nanomat. Chemical Physics Letters, 2018, 709: 77-81.
[16] *Chen Z, Vorobyeva E, Mitchell S, et al.* A heterogeneous single-atom palladium catalyst surpassing homogeneous systems for Suzuki coupling. Nature nanotechnology, 2018, 13(8): 702-707.
[17] *Luo M, Yin H.* Adsorption of NH_3 on Monolayer SiC Doped with Noble Metals: A First-Principles Study. Integrated Ferroelectrics, 2023, 231(1): 89-97.
[18] *Gui Y, Shi J, Xu L, et al.* Aun (n= 1–4) cluster doped $MoSe_2$ nanosheet as a promising gas-sensing material for C_2H_4 gas in oil-immersed transformer. Applied Surface Science, 2021, 541: 148356.
[19] *Dimcheva N.* Nanostructures of noble metals as functional materials in biosensors. Current Opinion in Electrochemistry, 2020, 19: 35-41.
[20] *Yan H, Cheng H, Yi H, et al.* Single-atom Pd1/graphene catalyst achieved by atomic layer deposition: remarkable performance in selective hydrogenation of 1,3-butadiene. Journal of the American chemical society, 2015, 137(33): 10484-10487.
[21] *Tao H, Choi C, Ding L X, et al.* Nitrogen fixation by Ru single-atom electrocatalytic reduction. Chem, 2019, 5(1): 204-214.
[22] *Lin J, Wang A, Qiao B, et al.* Remarkable performance of Ir_1/FeO_x single-atom catalyst in water gas shift reaction. Journal of the American Chemical Society, 2013, 135(41): 15314-15317.
[23] *Nikmanesh S, Safaiee R, Sheikhi M H.* Enhanced methane-sensing performances of Pd (monomer or dimer) decorated or doped γ-Graphyne: A DFT insight. Surfaces and Interfaces, 2022, 29: 101658.
[24] *Long M, Tang L, Wang D, et al.* Electronic structure and carrier mobility in graphdiyne sheet and nanoribbons: theoretical predictions. ACS nano, 2011, 5(4): 2593-2600.
[25] *Shahri S G, Roknabadi M R, Radfar R.* Spin-dependent structural, electronic and transport properties of armchair graphyne nanoribbons doped with single transition-metal atom, using DFT calculations. Journal of Magnetism and Magnetic Materials, 2017, 443: 96-103.
[26] *Zhao C, Zhou X, Xie S, et al.* DFT study of electronic structure and properties of N, Si and Pd-doped carbon nanotubes. Ceramics International, 2018, 44(17): 21027-21033.
[27] *Mashhadzadeh A H, Vahedi A M, Ardjmand M, et al.* Investigation of heavy metal atoms adsorption onto graphene and graphdiyne surface: a density functional theory study. Superlattices and Microstructures, 2016, 100: 1094-1102.
[28] *Seif A, López M J, Granja-DelRío A, et al.* Adsorption and growth of palladium clusters on graphdiyne. Physical Chemistry Chemical Physics, 2017, 19(29): 19094-19102.